

Parametric study of loudspeaker spacing in an active noise control headrest system with head-tracking

Chung Kwan Lai¹, Jordan Cheer Institute of Sound and Vibration Research, University of Southampton University Rd, SO17 1BJ, United Kingdom.

ABSTRACT

The integration of head-tracking can improve the performance of active noise control headrest systems, by enabling a reduction in the mismatch between the plant model used by the controller and the physical plant response to be realised. However, the performance may still be limited due to constraints on the resolution of head-tracking and previous work has shown that the robustness of the system then depends on both the initial head position and the direction of head movement. This paper builds on this previous work to explore how the spacing between the two loudspeakers used in the headrest influences the effective controller performance over the spatial region where the head position is tracked. It is shown, through numerical simulations, that a trade-off can be observed between the controller robustness and the spatial extent over which effective control is achieved. These findings may be used to inform the robust design of an active headrest system with head-tracking.

1. INTRODUCTION

An active headrest system operates on the principle of local sound control, aiming to create a localized zone of quiet around the listener's ears using secondary sources positioned behind the user [1, 2]. While local control methods provide extended control at higher frequencies compared to global control methods [3], the zone of quiet diminishes with increasing frequency, thereby limiting the maximum bandwidth available for effective control when head movements occur. To improve the achievable noise reduction during head movements, a head-tracker [4] can be utilised to update the plant model used in the control system based on the current head position, which allows the mismatch between the plant model and the physical plant response to be reduced. This improves control performance with respect to head movements and has therefore gained significant attention in the realisation of active headrest systems.

While it would be ideal for the plant model to be updated at head positions with the highest possible accuracy, the practicable level of accuracy is limited by the acceptable level of complexity associated with the calibration procedure and the corresponding length of calibration time. This means that errors between the physical response of the plant and the plant model may still be present, potentially degrading the control performance. Many studies have been conducted to

¹C.K.Lai@soton.ac.uk

better understand and improve the performance of head tracking equipped local active control systems. These can be categorised as investigations on the effect of tracking resolution during head movement [5, 6], improvements in the tracking ability of the head tracker [7], integration of interpolation strategies to improve accuracy between tracking grid points [8], or enhancements in the robustness of the control system against head tracking limitations [9]. However, it is also important to note that robust performance can be influenced by the initial head position within the tracking grid as well as the configuration of the active headrest, in particular, the distance between the two secondary loudspeakers. This behaviour is still not fully understood in head-tracking-equipped active headrests and is therefore explored in this paper. The structure of the paper is as follows: Section 2 presents the configuration of the active headrest system and the control strategy formulation; Section 3 examines the effect of tracking resolution on overall performance for two predefined headrest configurations corresponding to different loudspeaker spacings; Section 4 investigates the effect of the initial head position on robust performance; Section 5 presents a parametric study on the effect of loudspeaker spacing on robust performance in the presence of tracking error; and Section 6 draws conclusions.

2. CONFIGURATION OF THE ACTIVE HEADREST

Figure 1 presents a numerically simulated configuration for the active headrest, which utilizes a boundary element model of the KU100 head [10] implemented in COMSOL to represent the user's head. The setup includes two monopole sources with control signals u_1 and u_2 , representing the secondary loudspeakers positioned 2s apart in the active headrest, as well as 16 monopole sources placed 3 m away from the origin to simulate primary noise arriving from different directions. The plant responses from the primary and secondary sources to the error sensors are denoted by **P** and **G**, respectively. The secondary plant responses for each head position within a translational grid of (0.4×0.2) m were obtained during the initial calibration phase and were later used to update the plant model, $\hat{\mathbf{G}}$, based on the head position provided by the head-tracker. Assuming the disturbance signal is tonal, the cost function to be minimised by an unconstrained tonal controller shown in Figure 1a can be formulated in the frequency domain as

$$J = \mathbb{E}\left[\mathbf{e}^{\mathsf{H}}\mathbf{e} + \beta\mathbf{u}^{\mathsf{H}}\mathbf{u}\right] = \operatorname{tr}\left\{\mathbf{S}_{ee} + \beta\mathbf{S}_{uu}\right\},\tag{1}$$

where $\mathbb{E}\left[\cdot\right]$ and $\operatorname{tr}\left\{\cdot\right\}$ denote the expectation and trace operators, respectively; $(\cdot)^H$ represents the Hermitian transpose; β is the regularization parameter; and \mathbf{S}_{ee} and \mathbf{S}_{uu} are the complex spectral density matrices for the complex vector signals \mathbf{e} and \mathbf{u} , respectively, defined using the general notation $\mathbf{S}_{xy} = \mathbb{E}\left[\mathbf{y}\mathbf{x}^H\right]$. Under an ideal scenario where the plant model at the current head position is perfectly known, i.e. $\mathbf{G} = \hat{\mathbf{G}}$, the vector of optimal control signals driving the secondary sources is given by

$$\mathbf{u}_{opt} = -\left[\mathbf{G}^{\mathrm{H}}\mathbf{G} + \beta \mathbf{I}\right]^{-1}\mathbf{G}^{\mathrm{H}}\mathbf{d}.$$
 (2)

where I is the identity matrix. Since the assumed active headrest system, with two inputs and two outputs, presents a fully-determined system, the cost function from Equation (1) should theoretically be 0 under optimal control, provided that no regularization is introduced. However, the control performance can still degrade during head movement due to the finite head-tracking resolution imposed by limiting the calibration complexity, leading to errors between the physical plant response and the plant model, i.e. $G \neq \hat{G}$. In this work, the potential geometrical errors between the physical and modelled head positions are assessed for all possible head movements within the tracking grid, with a detailed analysis for individual movements along the sway (right) and surge (front, back) translational degrees of freedom, as illustrated in Figure 2. The pink cross in Figure 2 in each case denote the modelled head positions, and the coloured arrows denote the physical head positions corresponding to three different levels of the tracking error. Assuming that the degradation in the

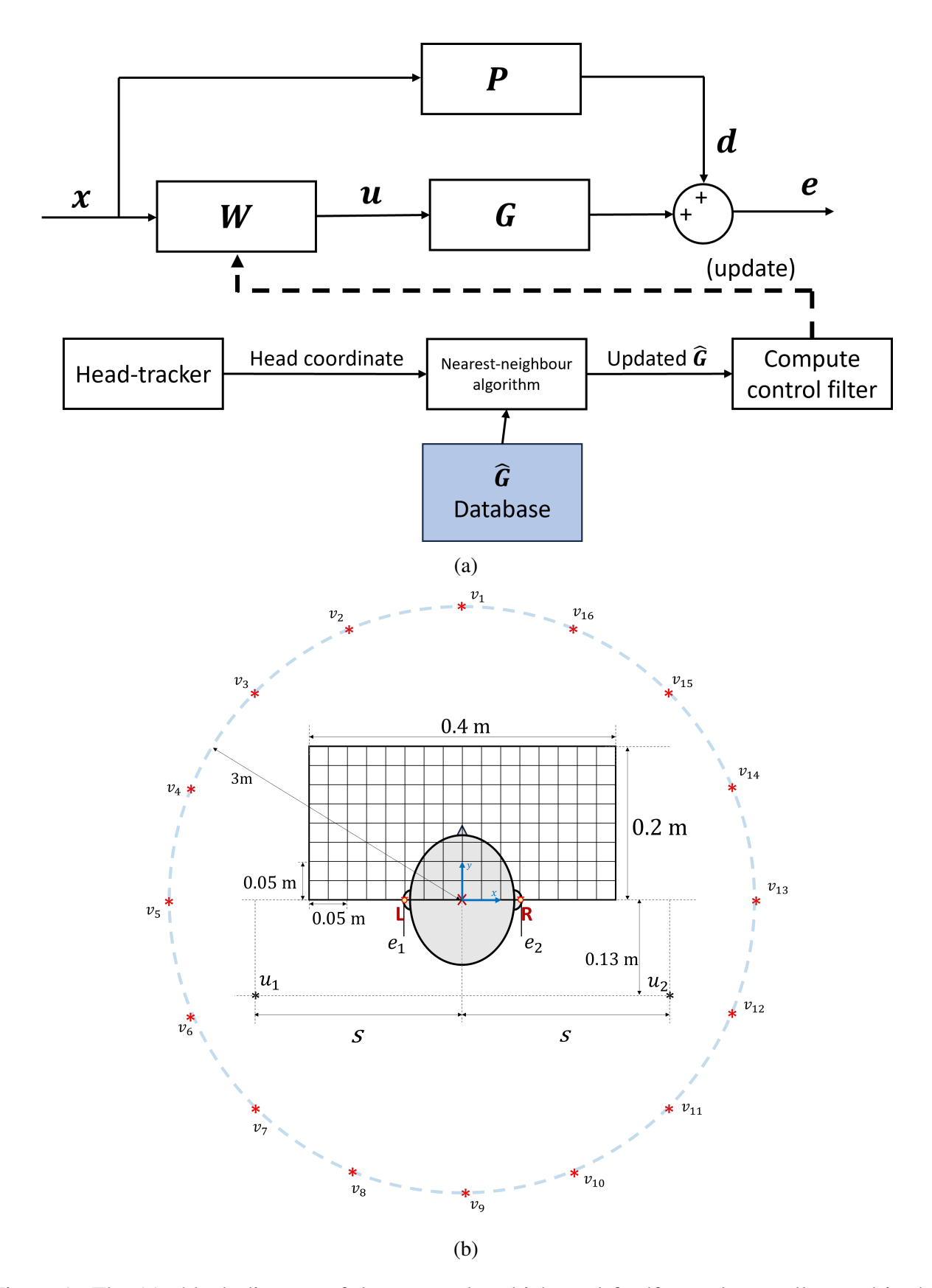


Figure 1: The (a): block diagram of the assumed multichannel feedforward controller used in the active headrest and (b): configuration of the active headrest where the head translates in the sway (left/right) and surge (front/back) directions within a (0.4×0.2) m translational grid. The minimum grid spacings for the translational grid are given by 0.025 m, and the distance between the two secondary loudspeakers is denoted by 2s.

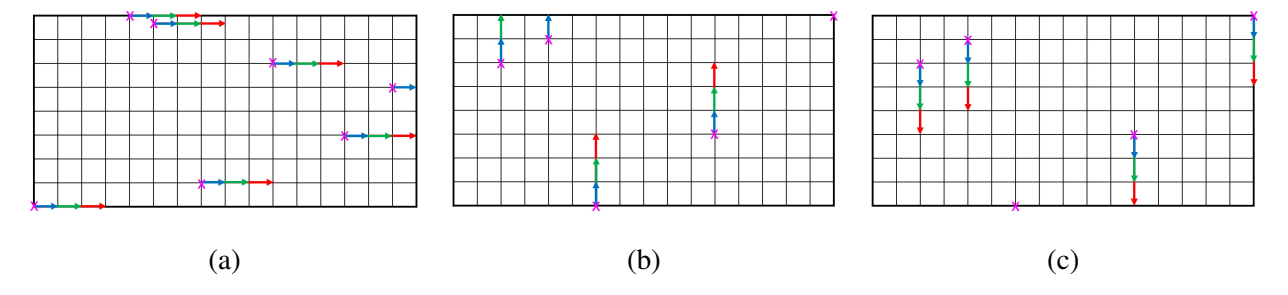


Figure 2: The potential errors between the physical and modelled head positions in the (a): sway (right), (b): surge (front) and (c): surge (back).

control performance is solely due to modelling error between the plant model and the physical plant response, the vector of control signals calculated using the plant model, $\hat{\mathbf{G}}$, and is given by

$$\mathbf{u}_{o} = -\left[\hat{\mathbf{G}}^{H}\hat{\mathbf{G}} + \beta \mathbf{I}\right]^{-1}\hat{\mathbf{G}}^{H}\mathbf{d}.$$
 (3)

The spectral density matrix of the signals at the error microphones after control using Equation (3) can then be obtained as

$$\mathbf{S}_{ee} = \mathbf{S}_{dd} - \mathbf{S}_{dd}\hat{\mathbf{G}} \left(\hat{\mathbf{G}}^{H}\hat{\mathbf{G}} + \beta \mathbf{I}\right)^{-1} \mathbf{G}^{H} - \mathbf{G} \left(\hat{\mathbf{G}}^{H}\hat{\mathbf{G}} + \beta \mathbf{I}\right)^{-1} \hat{\mathbf{G}}^{H} \mathbf{S}_{dd} + \mathbf{G} \left(\hat{\mathbf{G}}^{H}\hat{\mathbf{G}} + \beta \mathbf{I}\right)^{-1} \hat{\mathbf{G}}^{H} \mathbf{S}_{dd} \hat{\mathbf{G}} \left(\hat{\mathbf{G}}^{H}\hat{\mathbf{G}} + \beta \mathbf{I}\right)^{-1} \mathbf{G}^{H},$$

$$(4)$$

where $\mathbf{S}_{dd} = \mathbf{P}\mathbf{S}_{vv}\mathbf{P}^{H}$, with \mathbf{S}_{vv} defined as an identity matrix to model incoherent primary sources as depicted in Figure 1b. Equation (4) is then used to compute the attenuation performance for the overall active headrest system, which is given by

$$L_e = -10\log_{10} \left| \frac{\operatorname{tr} \{ \mathbf{S}_{ee} \}}{\operatorname{tr} \{ \mathbf{S}_{dd} \}} \right| \tag{5}$$

and the attenuation performance at the *i*-th ear is given by

$$L_{e_i} = -10\log_{10} \left| \frac{S_{e_i e_i}}{S_{d_i d_i}} \right|. \tag{6}$$

3. EFFECT OF TRACKING RESOLUTION ON THE CONTROL PERFORMANCE FOR THE TWO PRE-DEFINED HEADREST CONFIGURATIONS

In this section, two headrest configurations with different loudspeaker spacings, that is, s = 0.1375 m for the narrow-spacing configuration and s = 0.275 m for the wide-spacing configuration, are used to compare the effect that the tracking error has on the control performance. Figure 3 shows the plot of the overall attenuation performance, as computed from Equation (5), for various types of plant modelling error, tracking resolution and loudspeaker configurations. As perhaps expected, the results in general show that the averaged attenuation level for all cases, as represented by the line plots, increases as the tracking resolution increases. However, it can be seen that the averaged attenuation performance differs between the wide- and narrow-spaced configurations across different degrees of freedom. Additionally, the range of the overall attenuation performance among all possible tracking errors, as indicated by the error bars and the shaded regions, also varies between the two configurations. Taking the case of sway movement as an example, the shaded region for the wide-spacing configuration in Figure 3b remains relatively narrow, ranging between 3–5 dB at all frequencies. In contrast, the shaded region for the narrow-spacing configuration in Figure 3 exhibits a much wider range of approximately 15 dB. Physically, this indicates a greater variance in attenuation

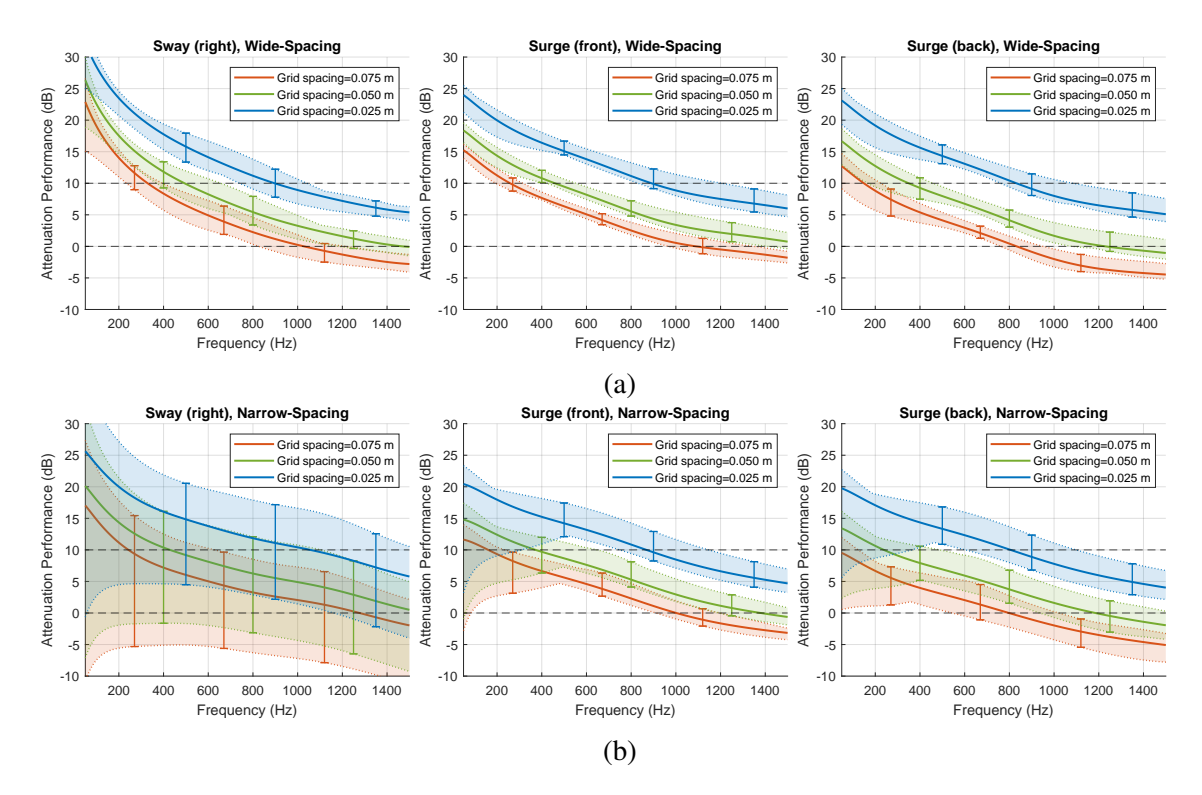


Figure 3: The overall attenuation performance computed according to Equation (5) plotted against frequency when the plant modelling error is present for the (a): wide-spacing configuration (s = 0.275 m) and (b): narrow-spacing configuration (s = 0.1375 m). The line plots represent the overall attenuation performance averaged across all possible head movements, and the shaded regions/error bars indicate the range in the performance for all head movements.

performance between different combinations of sway movements, where some combinations maintain consistently high attenuation across frequencies, while others experience attenuation levels below 10 dB throughout. This general trend in behaviour also applies for surge movements, although the range for the narrow-spaced configuration for surge movement is much narrower than that for the case for sway movements. Interestingly, it is found that the attenuation performance for backward surge movements, across all tracking resolutions and loudspeaker spacings, is generally lower than for forward surge movements, highlighting an asymmetric degradation in control performance depending on the direction of the tracking error.

Based on the shaded regions shown in Figure 3, it can be deduced that the control performance in the presence of tracking error is influenced by the initial head position. As head-tracking techniques should ideally enable high attenuation performance across all head positions, it is of interest to explore how tracking error reduces the spatial extent over which effective control is achieved. Figure 4 shows the percentage of head movements, out of all possible head movements within the tracking grid for a given type of head movement and tracking resolution, that achieve an attenuation performance level of at least 10 dB across the considered frequency range. For both headrest configurations, decreasing the tracking resolution results in a lower percentage value for all types of head movement, which is consistent with the findings of Figure 3. Furthermore, the results demonstrated a significant difference in the percentage of head movements achieving the 10 dB attenuation performance threshold when assessed for individual microphones, as given in Equation (6), compared to the overall system, as in Equation (5). These differences depend on the type of head movement and the headrest configuration. For sway movements in the wide-spacing configuration with a tracking resolution of 2.5 cm, the percentage associated with the attenuation performance at the left and right error microphones, which is indicated by the dotted and dashed plots, respectively, is less than 100% at around 600 Hz and decreases to 25% at 1500 Hz. In contrast, the percentage for the overall attenuation performance, as

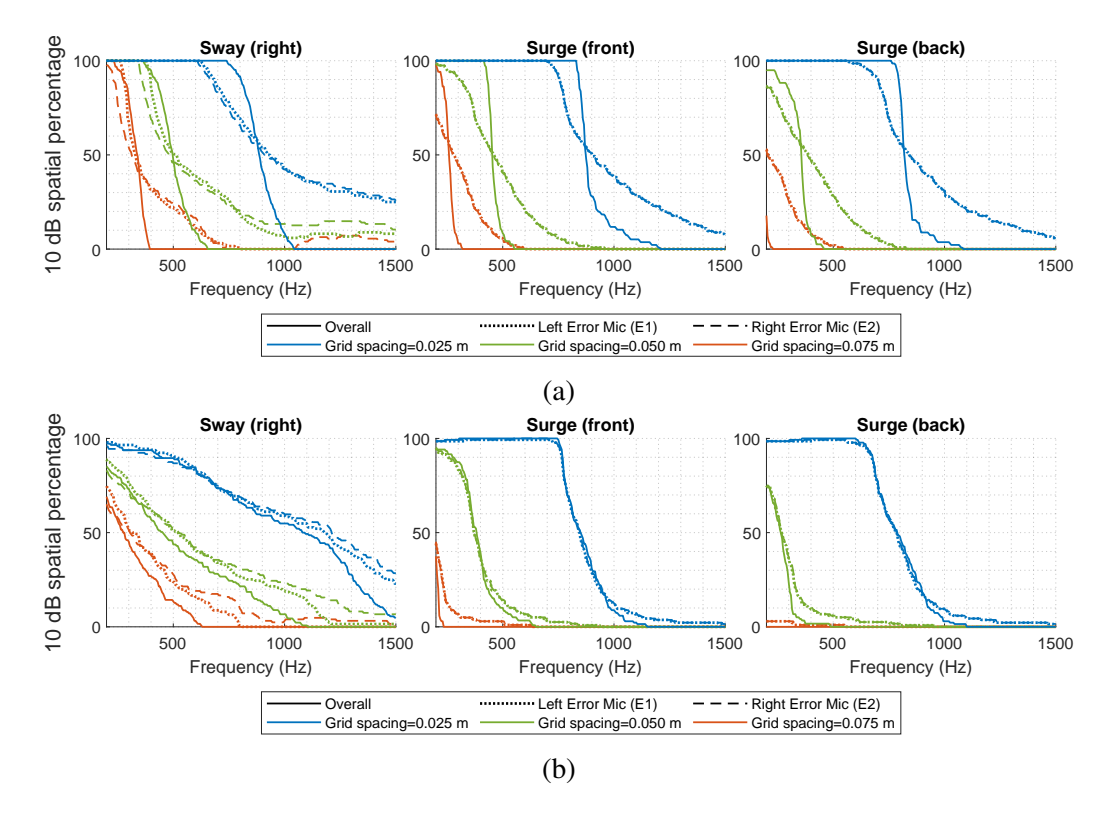


Figure 4: The percentage of all head movements for which an attenuation performance level of at least 10 dB is achieved for the (a): wide spacing configuration and (b): narrow spacing configuration for different tracking resolution and types of head movement.

represented by the solid line, falls below 100% at a higher frequency, around 750 Hz, but then declines more rapidly, reaching 0% at approximately 1050 Hz. While this observed behaviour is consistent for forward and backward surge movements in the wide-spacing configuration, it does not apply to the results shown for the narrow-spacing configuration in Figure 4b, where a small difference is observed in the percentage plots between the overall system and the individual ears. While the percentage for the 2.5 cm resolution in the case of sway movements in the narrow-spacing configuration is generally higher than in the wide-spacing configuration, a trade-off is observed: the percentage for the narrow-spacing configuration does not reach 100% even at low frequencies, and this shows how the headrest configuration influences the spatial range over which effective control is achieved for certain types of tracking error.

4. EFFECT OF INITIAL HEAD POSITION AND THE DIRECTION OF TRACKING ERROR ON THE CONTROL PERFORMANCE FOR THE TWO PRE-DEFINED HEADREST CONFIGURATIONS

To understand how the initial head position influences the attenuation performance, it would be useful to examine the cut-off frequencies where the attenuation performance level first crosses below 10 dB for each head position. Figure 5 and Figure 6 show the colour plots illustrating the frequency at which the attenuation level, evaluated for the individual ear and the overall system, first crosses below 10 dB. These colour plots, generated for the finest tracking resolution of 2.5 cm, are mapped to each initial head position within the tracking grid described in Figure 1b and correspond to the wide- and narrow-spaced configurations, respectively. For all types of tracking errors in the wide spacing configuration shown in Figure 5, a mismatch in the cut-off frequency between the left and right ears is observed, and this mismatch depends on the type of tracking error and the initial head position. For instance, in the case of sway movements, as shown in Figure 5a, the 10 dB cut-off frequency exceeds 1500 Hz in the region $-0.2 \le x \le -0.125$ m and decreases towards the positive x-direction. In contrast, for

the right error microphone, this frequency exceeds 1500 Hz in the region $0.075 \le x \le -0.2$ m and decreases along the negative *x*-direction. However, the cut-off frequency evaluated for the overall attenuation performance shows increased uniformity across the tracking grid at around 900 Hz. A similar mismatch behaviour was also observed for forward and backward surge errors, as shown in Figure 5b and Figure 5c. However, in these cases, the 10 dB cut-off frequency exceeds 1500 Hz near (0, 0.2) m and (0, -0.2) m for the left and right ears, respectively, and decreases diagonally upwards. Additionally, in the case of backward surge, a region with a cut-off frequency below 650 Hz is observed near $(\pm 0.175, 0.025)$ m for the left and right error microphones, highlighting an asymmetry in control performance depending on the direction of the tracking error.

The mismatch in the attenuation performance between the left and right ears behaves differently in the narrow-spaced configuration, as shown in Figure 6. For the case of sway movements, as shown in Figure 6a, the overall attenuation performance exhibits a higher cut-off frequency of around 1300 Hz at the central region, because the high cut-off frequency region for both the left and right error microphones is also located in the central region. Additionally, this cut-off frequency decreases diagonally downwards to 200 Hz and below as it gets closer to (0.175,0) m and (-0.2,0) m, illustrating a reduced spatial extent where control that is robust to sway movement is achieved. In the case of forward surge movements, as shown in Figure 6b, the cut-off frequency for the left and right error microphones is around 800 Hz for most head positions. However, it increases to approximately 1100 Hz at (-0.125, 0) m for the left microphone and (+0.125, 0) m for the right microphone. At (-0.2, 0) m, it exceeds 1500 Hz for the left microphone, while the same occurs at (+0.2, 0) m for the right microphone. The case of backward surge movements, shown in Figure 6c, exhibits similar behaviour to forward surge movements, except that the cut-off frequency near (±0.025,0) m is lower than in the forward surge case. Additionally, the cut-off frequency for the left and right error microphones is below 200 Hz for initial head positions of (0.2, 0.0025) m and (-0.2, 0.0025) m, respectively. This is consistent with the observation made for the wide-spaced configuration, where control performance exhibits asymmetry depending on the direction of the tracking error.

The results from Figure 5 and Figure 6 have highlighted a potential mismatch in the attenuation performance between the left and right error microphones under the presence of tracking error. To allow better visualisation in this mismatch, Figure 7 presents the attenuation performance as a function of frequency for two initial head positions with a tracking error in the sway direction for the two headrest configurations. For the initial head position at (0, 0.05) m, shown in Figure 7a, attenuation levels for the left and right error microphones under the wide-spaced configuration (solid lines) remain similar across all frequencies. However, when the initial position of the head is (0.1, 0.05) m, as shown in Figure 7b, the attenuation level at the right error microphone is consistently higher than at the left, and this difference increases with frequency. This suggests that at higher frequencies, while robust performance is maintained at the right error microphone, the left error microphone experiences a significant degradation in control performance. A different mismatch behaviour is observed for the narrow-spaced configuration (dashed lines). Although there is a mismatch in attenuation levels between the right and left error microphones at the initial head position of (0, 0.05) m, it remains relatively constant across frequencies, and the overall attenuation performance is consistently higher than in the wide-spacing configuration. However, this behaviour does not hold for the initial head position of (0.1, 0.05) m, highlighting the influence of the spacing of the loudspeakers and the initial head position on robust performance and attenuation mismatch between the two microphones.

5. PARAMETRIC STUDY ON THE EFFECT OF LOUDSPEAKER'S SPACING ON THE CONTROL PERFORMANCE

This section presents a parametric study examining the effect of loudspeaker spacing on robust performance in the presence of tracking error by varying the source spacing parameter *s* from 0.0125 m to 0.5 m in increments of 0.0125 m. Building on the plot shown in Figure 4, Figure 8 presents a contour plot illustrating the percentage of considered head movements under which an

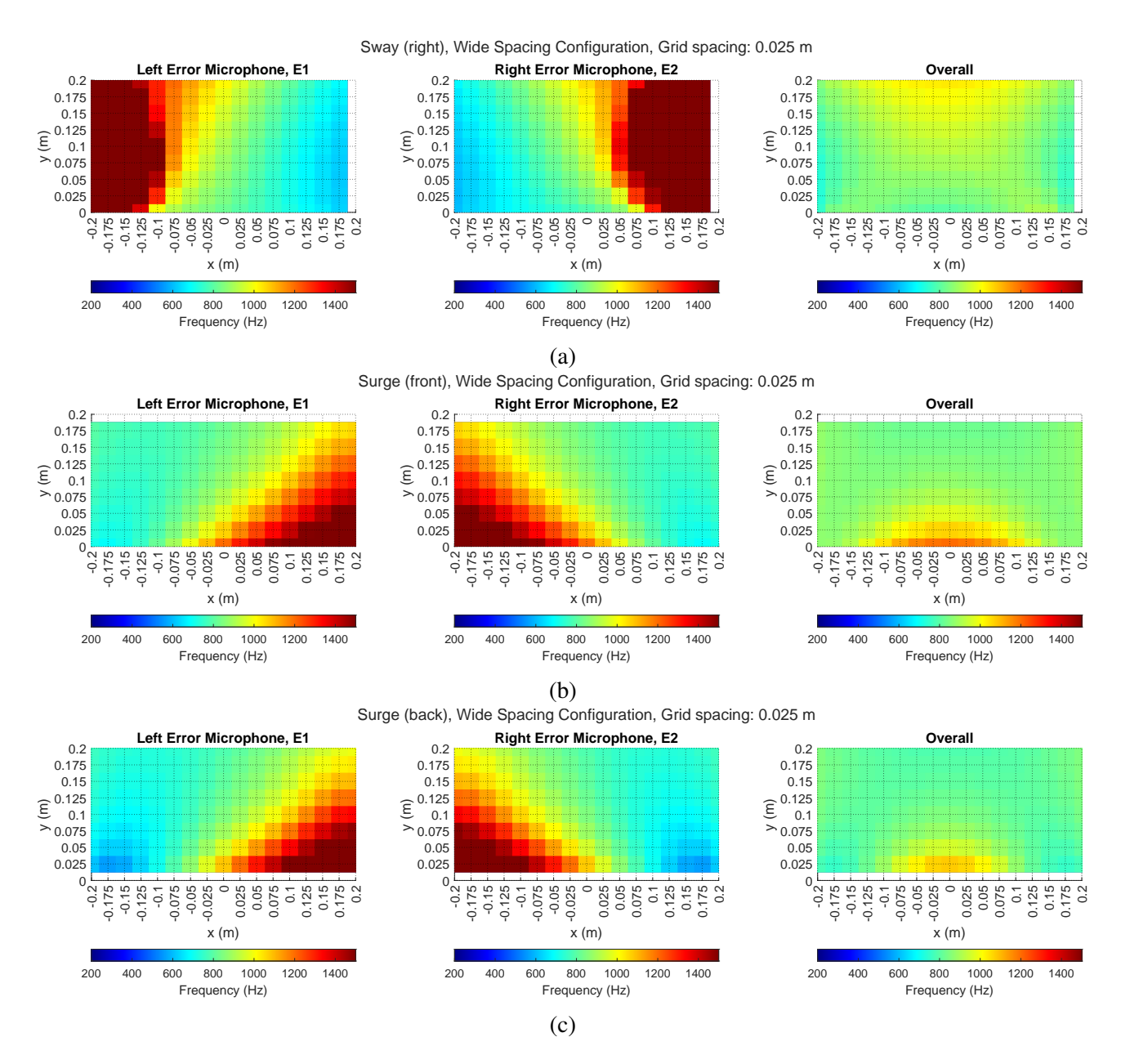


Figure 5: The colour plots showing the frequency at which the attenuation level first crosses below 10 dB for head movements in the (a): sway (right), (b): surge (front) and (c): surge (back) direction, mapped to the initial head positions for the wide spacing configuration. The unfilled regions represent initial head positions where head movement within the specified grid is infeasible.

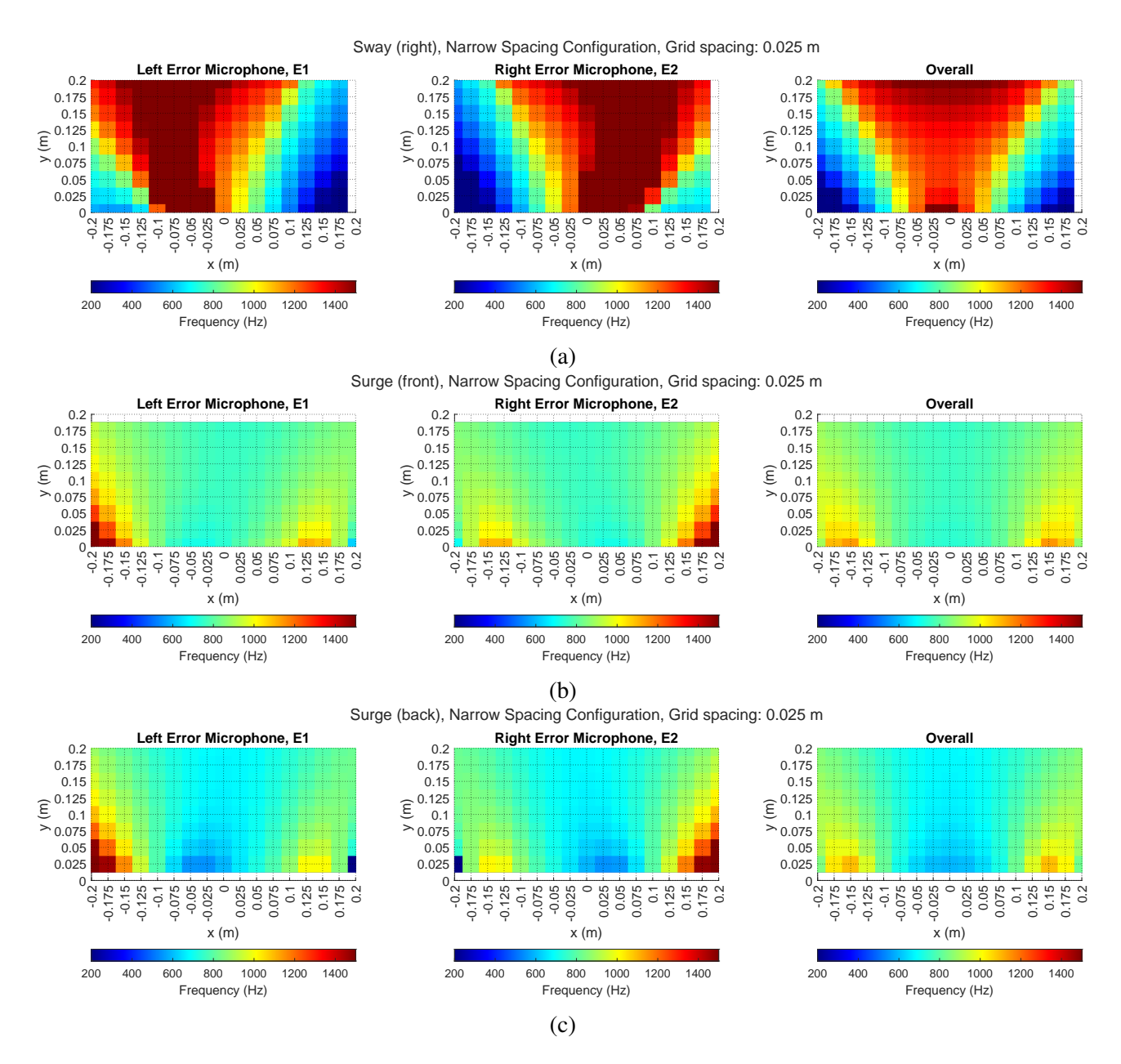


Figure 6: The colour plots showing the frequency at which the attenuation level first crosses below 10 dB for head movements in the (a): sway (right), (b): surge (front) and (c): surge (back) direction, mapped to the initial head positions for the narrow spacing configuration. The unfilled regions represent initial head positions where head movement within the specified grid is infeasible.

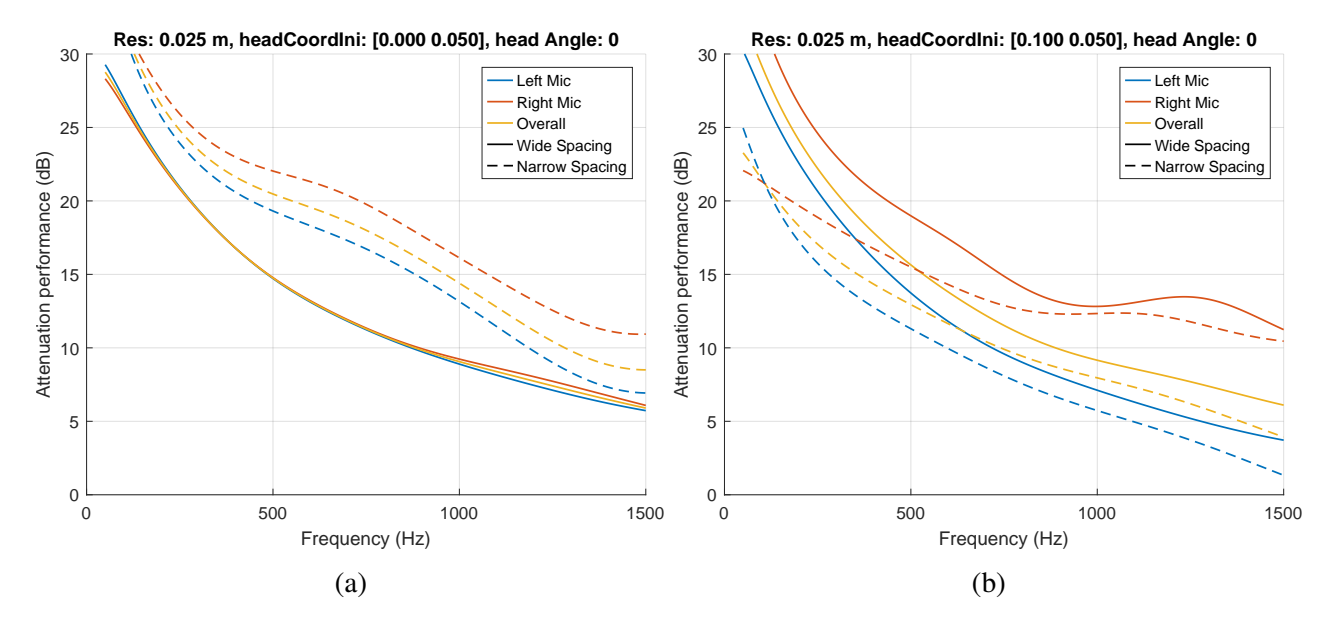


Figure 7: Attenuation performance plots for the individual microphone and the overall system for the two headrest configurations, shown for sway movement with a tracking resolution of 0.025 m, at initial head positions of (a): (0, 0.05) m and (b): (0.1, 0.05) m.

attenuation performance of at least 10 dB is achieved across frequency for different loudspeaker spacings. Based on these results, it can be seen that the trade-off between the maximum frequency at which control performance exceeds 10 dB and the spatial extent over which this level of control is achieved depends on loudspeaker spacing as well as the direction of tracking error. For sway movements, as shown in Figure 8a, a source spacing of s = 0.3 m allows robust control to be achieved up to 650 Hz for all head positions, which is the highest amongst all spacing options for both the left and right error microphones. However, due to the mismatch in attenuation performance between the left and right microphones, the overall performance percentage drops rapidly to 0% at around 1 kHz, a trend that remains consistent for $0.3 \le s \le 0.5$ m. In contrast, a source spacing of s = 0.1 m enables effective control to be achieved up to 1100 Hz for at least 50% of sway movements, but at the cost of a reduced spatial range over which effective control is maintained across all frequencies. This trade-off, however, is not observed for the case of surge movements shown in Figure 8b and Figure 8c, where it is found that increasing source spacing beyond s = 0.3 m generally increases the maximum frequency where the percentage remains 100% as well as the maximum frequency where effective control is achieved for at least 50% of surge movements. These findings highlight the distinct influence of loudspeaker spacing on robust control performance, demonstrating that optimal spacing depends on both the frequency range and the specific type of tracking error.

6. CONCLUSIONS

Although the integration of head-tracking techniques into active noise control headrest systems allows a potential improvement in the achievable noise reduction, performance may still be limited due to constraints on head-tracking resolution. The degradation in control performance is dependent on the initial head position, the direction of tracking error, and the loudspeaker spacing utilised in the active headrest system. These behaviours are explored in this paper by first investigating the effect of tracking resolution on the performance of the overall system, followed by investigating the effect of initial head position as well as the direction of tracking error for narrow-spaced and wide-spaced headrest configurations. Finally, a parametric study of loudspeaker spacing is conducted under the influence of tracking error to better quantify the trade-off observed between robust performance and the spatial extent over which effective control is achieved.

The findings of this work demonstrate how tracking resolution across different directions of

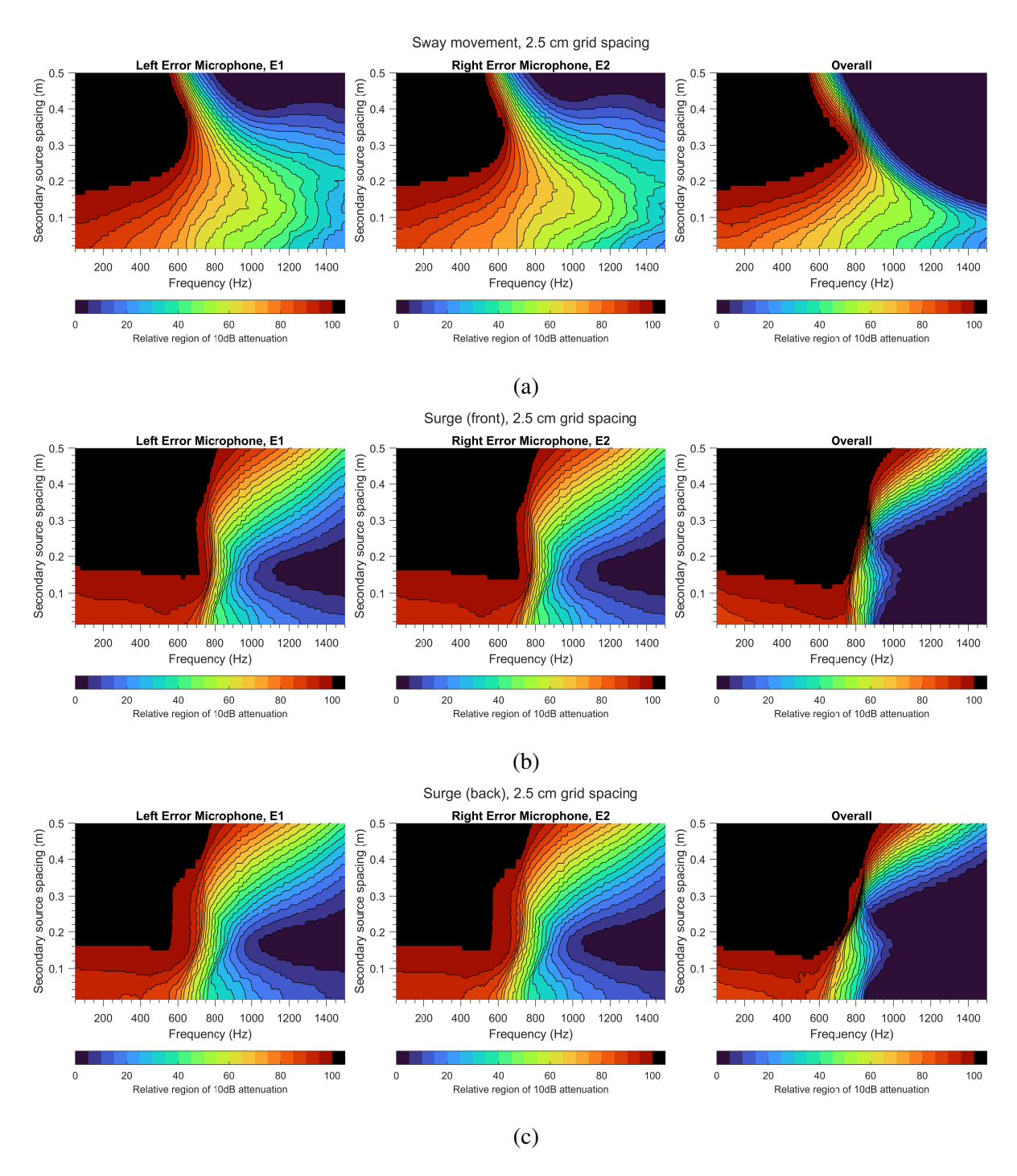


Figure 8: The colour plots showing the percentage of all head movements for which an attenuation performance of at lesat 10 dB is achieved, presented for different loudspeaker spacings, when tracking errors are introduced in the direction of (a): sway (right), (b): surge (front), and (c): surge (back).

tracking error affects control performance differently for each ear, leading to a mismatch in the attenuation performance that depends on the initial head position and the loudspeaker's spacing. The results presented in this paper may be used to inform the robust design of an active headrest system with head-tracking, although further research is required to optimise the trade-off between the size of the tracking grid, loudspeaker spacing, and control robustness. Future work could also explore interpolation strategies [8] to minimise the tracking error, as well as perceptual evaluations to assess the impact of attenuation mismatch between the ears on listener experience.

ACKNOWLEDGMENTS

The work was supported by the project IN-NOVA: Active reduction of noise transmitted into and from enclosures through encapsulated structures, which has received funding from the European Union's Horizon Europe programme under the Marie Sklodowska-Curie grant agreement no. 101073037. This work was funded by UK Research and Innovation under the UK government's Horizon Europe funding guarantee [grant number EP/X027767/1]. JC's time was supported by the Department of Science, Innovation and Technology (DSIT) Royal Academy of Engineering under the Research Chairs and Senior Research Fellowships programme.

REFERENCES

- 1. Harry F. Olson and Everett G. May. Electronic Sound Absorber. *The Journal of the Acoustical Society of America*, 25(6):1130–1136, November 1953.
- 2. B. Rafaely, S. J. Elliott, and J. Garcia-Bonito. Broadband performance of an active headrest. *The Journal of the Acoustical Society of America*, 106(2):787–793, August 1999.
- 3. P. A. Nelson, A. R. D. Curtis, S. J. Elliott, and A.J. Bullmore. The active minimization of harmonic enclosed sound fields, part I: Theory. *Journal of Sound and Vibration*, 117:1–13, 1987. Read_Status: Done Read_Status_Date: 2024-09-20T11:56:06.290Z.
- 4. Stephen J. Elliott, Woomin Jung, and Jordan Cheer. Head tracking extends local active control of broadband sound to higher frequencies. *Scientific Reports*, 8(1):1–7, December 2018.
- 5. Hao Jiang, Hongyu Chen, Jiancheng Tao, Haishan Zou, and Xiaojun Qiu. Accuracy requirements of ear-positioning for active control of road noise in a car. *Applied Acoustics*, 225:110164, November 2024. Read_Status: Done Read_Status_Date: 2024-11-11T22:45:18.126Z.
- 6. Chung Kwan Lai, Jordan Cheer, and Chuang Shi. The effect of head-tracking resolution on the stability and performance of a local active noise control headrest system. *The Journal of the Acoustical Society of America*, 157(2):766–777, February 2025.
- 7. Yuteng Liu, Haowen Li, Haishan Zou, Zhibin Lin, and Jing Lu. Active headrest combined with a depth camera-based ear-positioning system. *The Journal of the Acoustical Society of America*, 157(1):519–526, January 2025.
- 8. Jun Young Oh, Hyun Woo Jung, Myung Han Lee, Kyoung Hoon Lee, and Yeon June Kang. Enhancing active noise control of road noise using deep neural network to update secondary path estimate in real time. *Mechanical Systems and Signal Processing*, 206:110940, January 2024. Read_Status: Done Read_Status_Date: 2024-10-16T20:57:28.691Z.
- 9. Hongyu Chen, Xiaofan Huang, Haishan Zou, and Jing Lu. Research on the Robustness of Active Headrest with Virtual Microphones to Human Head Rotation. *Applied Sciences*, 12(22):11506, November 2022. Read_Status: Done Read_Status_Date: 2024-10-19T15:23:23.516Z.
- Fabio Di Giusto, Sjoerd Van Ophem, Wim Desmet, and Elke Deckers. Analysis of laser scanning and photogrammetric scanning accuracy on the numerical determination of Head-Related Transfer Functions of a dummy head. Acta Acustica, 7:53, 2023.